A cryostat and temperature control system optimized for measuring relaxations of glass-forming liquids

Igarashi, Brian; Christensen, Tage Emil; Larsen, Ebbe Hyldahl; Olsen, Niels Boye; Pedersen, Ib Høst; Rasmussen, Torben Steen; Dyre, J. C.

Published in:
Review of Scientific Instruments

DOI:
10.1063/1.2903419

Publication date:
2008

Document Version
Publisher's PDF, also known as Version of record

Citation for published version (APA):
Igarashi, B., Christensen, T. E., Larsen, E. H., Olsen, N. B., Pedersen, I. H., Rasmussen, T. S., & Dyre, J. C. (2008). A cryostat and temperature control system optimized for measuring relaxations of glass-forming liquids. *Review of Scientific Instruments*, *79*(4). https://doi.org/10.1063/1.2903419

A cryostat and temperature control system optimized for measuring relaxations of glass-forming liquids

Brian Igarashi, Tage Christensen, Ebbe H. Larsen, Niels Boye Olsen, Ib H. Pedersen, Torben Rasmussen, and Jeppe C. Dyre
DNRF centre "Glass and Time," IMFUFA, Department of Sciences, Roskilde University, P.O. Box 260, DK-4000 Roskilde, Denmark

(Received 16 November 2007; accepted 9 March 2008; published online 11 April 2008)

An experimental setup, including a cryostat and a temperature control system, has been constructed to meet the demands of measuring linear and nonlinear macroscopic relaxation properties of glass-forming liquids in the extremely viscous state approaching the glass transition. In order to be able to measure such frequency-dependent response functions accurately (including dielectric permittivity, specific heat, thermal expansivity, and shear and bulk moduli), as well as nonlinear relaxations following a temperature jump, one must have the ability to hold temperatures of liquids steady over the span of several days or even several weeks. To maximize temperature stability, special care is taken to thermally isolate the sample chamber of the cryostat. The main temperature control system is capable of maintaining temperatures within a few millikelvins. If liquid is deposited into a special transducer assembly that includes a subcryostat unit, the temperature of liquids can be maintained even more precisely, within a few tenths of a millikelvin. This subcryostat unit is more responsive to temperature changes because (i) it is equipped with a Peltier element that provides secondary heating and cooling, (ii) the transducer contains a layer of liquid that is only 50 μm thick, and (iii) feedback proportional-integral-derivative temperature control is implemented by a fully analog circuit. The subcryostat permits us to change and stabilize temperatures quickly; it takes only 10 s to stabilize the temperature within tenths of a millikelvin after a jump of 1 K, for example, a capability that is highly advantageous for accurately observing relaxation processes following a temperature step. © *2008 American Institute of Physics.* [DOI: 10.1063/1.2903419]

I. INTRODUCTION

It is now widely recognized that the glassy state is universal in the sense that any liquid may be brought into this state if cooled rapidly enough to avoid crystallization. One may speak of glass as the fourth state of conventional matter.[1] Within the last 15 years, the study of highly viscous liquids approaching the glass transition became a major research area within condensed matter physics and chemistry. The increased focus on glasses and glass-forming liquids was catalyzed by the fact that important problems remain unsolved,[2–10] with no consensus in sight regarding fundamental scientific questions such as the following: What is the origin of the rapidly increasing viscosity (where upon cooling one usually observes a much more dramatic increase than predicted by the well-known Arrhenius equation)? Why are simple exponential relaxations so rare and what is the origin of the observed relaxation time distributions?

These questions relate to the metastable supercooled liquid above the glass transition. Since glass is formed from a liquid, a better understanding of glass properties is expected to come from a better understanding of the highly viscous liquid phase preceding glass formation. Many papers have been published reporting molecular structure and dynamics monitored by static or dynamic neutron, x-ray, or light scattering measurements of glass-forming liquids held together by covalent, metallic, van der Waals, hydrogen, or ionic chemical bonds. Macroscopic properties such as specific heat monitored by differential scanning calorimetry and dielectric relaxation have also been subjects of intense interest.

A characteristic feature of highly viscous liquids approaching the glass transition is their very long relaxation times. Whereas, for instance, ambient water has a relaxation time in the picosecond range, glass-forming liquids have relaxation times that may exceed 1 s. The relaxation time increases quickly upon cooling, and the glass transition is the falling out of equilibrium taking place when the liquid relaxation time exceeds the laboratory time scale, thus inhibiting the liquid from coming to equilibrium. These extremely long relaxation times imply that well-known thermodynamic linear response properties such as specific heat and expansion coefficients all become frequency dependent at low frequencies (millihertz to kilohertz, depending on temperature).

Linear thermoviscoelasticity deals with frequency dependences of thermodynamic properties and their couplings to frequency-dependent mechanical properties. It is understood that, in principle, only infinitesimal perturbations are applied, thus ensuring linearity. Altogether, there are 12 linear thermoviscoelastic frequency-dependent response functions[11] (for example, isochoric specific heat, isobaric specific heat, isothermal compressibility, adiabatic compressibility, isobaric expansion coefficient, adiabatic contraction coefficient, isochoric pressure coefficient, and adiabatic pressure coefficient). By various theoretical arguments including Onsager reciprocity, it may be shown that only three of these response functions are independent.[12] Despite the classical

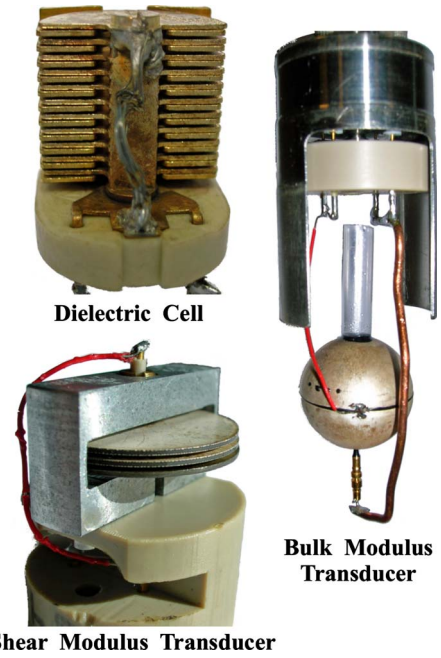

FIG. 1. (Color online) Examples of transducers used to measure response functions of viscoelastic glass-forming liquids. Liquid samples are inserted between 11 plates of the dielectric cell, between three plates of the piezoceramic shear modulus transducer, or inside a spherical shell of the piezoceramic bulk modulus transducer.

nature of the thermoviscoelastic response functions, there are still no reliable means of measuring any set of three independent response functions. Presently, we are developing techniques for performing such measurements, techniques that principally convert the problem of measuring a given property into measuring a frequency-dependent electrical impedance.

Several response functions may be measured by measuring electrical impedances or, more specifically, complex frequency-dependent capacitances of liquid-filled transducers. The dielectric permittivity of a liquid is measured by depositing a small quantity between plates of a dielectric cell (Fig. 1) and then measuring electrical capacitance of the cell. This is a standard technique, but perhaps less well known is that mechanical properties (bulk and shear moduli) of liquids

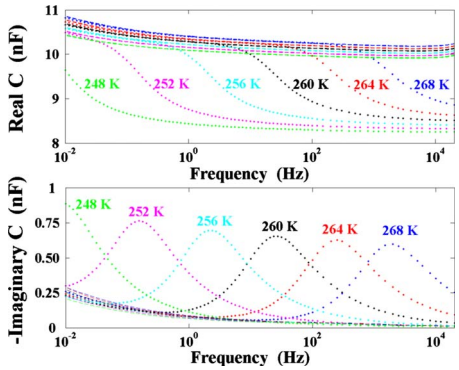

FIG. 2. (Color online) Typical measurements of the electrical capacitance of a piezoceramic shear modulus transducer. At each indicated temperature, data are shown for the two cases of when the transducer is empty (dashed curves) and when it is filled with five-ring polyphenyl ether diffusion pump oil (dotted curves). From these data, the shear modulus can be calculated using techniques described in Ref. 14.

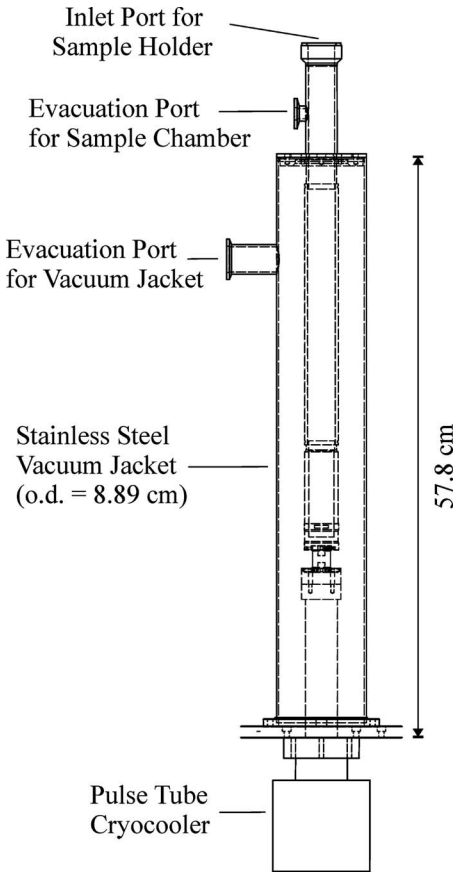

FIG. 3. Exterior features of the main cryostat.

also can be detected by measuring capacitances of liquid-filled piezoceramic transducers (Fig. 1).[13,14] From a general perspective, these piezoceramic transducers act like ordinary capacitors in that silver platings on the inner and outer surfaces of the spherical shell or on the top and bottom of each disk of the shear modulus transducer function as a pair of electrodes separated by a small distance (on the order of 0.5 mm); however, the transducers also possess extra capacitance originating from the piezoelectric nature of the material. When a liquid is in contact with the shell or disk, it inhibits this motion and, thereby, partially cancels the extra capacitance due to the piezoelectric effect. We thereby determine the stiffness or shear modulus of a liquid by measuring reduction of the electrical capacitance of a piezoceramic transducer that is caused by the liquid's presence.

An example of data taken with the shear modulus transducer is shown in Fig. 2. This graph illustrates how the real part of the capacitance is affected by the liquid. At low frequencies, liquid molecules have sufficient time to adjust their positions in response to shear stresses, and they do not significantly restrict motion of the piezoceramic disks; however, at higher frequencies, the liquid exhibits solidlike behavior and it opposes motion of the plates, thereby reducing the piezoelectric contribution to capacitance. (At frequencies corresponding to inverse liquid relaxation times, a peak occurs in the negative imaginary part of the capacitance, indicating where energy loss per cycle due to motion of liquid molecules is maximized.) In order to accurately measure the reduction of capacitance, we need to replicate experimental

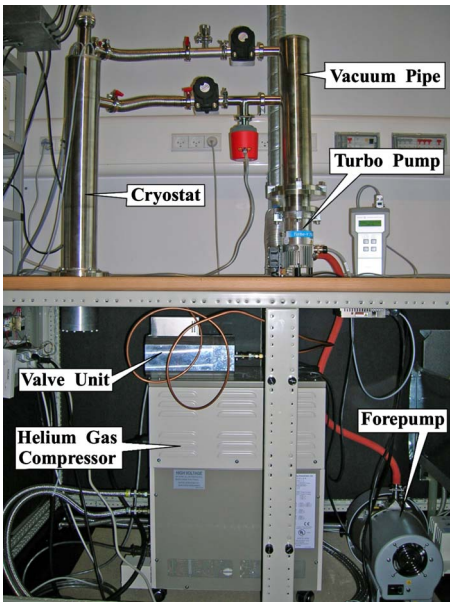

FIG. 4. (Color online) Pulse tube cryocooler and vacuum equipment for the main cryostat system. Compressed helium gas feeds into the valve unit, which then passes compressed gas to a coldhead mounted near the bottom of the main cryostat (appearing on the left-hand side of the photograph). Equipment underneath the laboratory bench normally is hidden behind insulated doors (not shown) to reduce noise.

conditions for the two cases of when the transducer is empty and when it is filled with liquid. Therefore, two requirements of the measurements are the following: (i) We must be able to set the temperature in a repeatable fashion and hold the temperature steady during a measurement and (ii) voltages applied to a transducer must be reproducible. The cryostat, subcryostat, and two temperature control systems described in this article are designed to meet the first requirement. The second requirement is an issue that is addressed in a companion article[15] that describes custom-built equipment used to measure electrical capacitances of transducers.

II. MAIN CRYOSTAT AND TEMPERATURE CONTROL SYSTEM

The temperature of the sample chamber in the cryostat (Figs. 3–6) is regulated by balancing heat injected into the chamber from a current-carrying coil of wire against heat removed by a cryocooler. Simultaneously heating and cooling the chamber this way allows us to change the temperature quickly. When conducting experiments on a liquid, it sometimes is necessary raise its temperature quickly by several degrees (for example, to avoid crystallization). It also is important to quickly make small changes in temperature for temperatures can be held steady only if minor corrections can be implemented quickly.

The setup described below has a couple of noteworthy features.

- Careful attention is paid to thermal isolation of the sample chamber of this cryostat; for example, the chamber is supported solely by thin-walled stainless steel tubes and a bellows hose in an effort to minimize conduction of heat.
- The temperature control system is capable of holding temperatures steady within a few millikelvins over the span of several days or even several weeks [for example, see Fig. 9(a) in Sec. III below]. This high stability is realizable only if temperatures of sensing electronic circuits themselves are stabilized. To this end, critical electronic components are mounted in an enclosure with a well-regulated temperature.

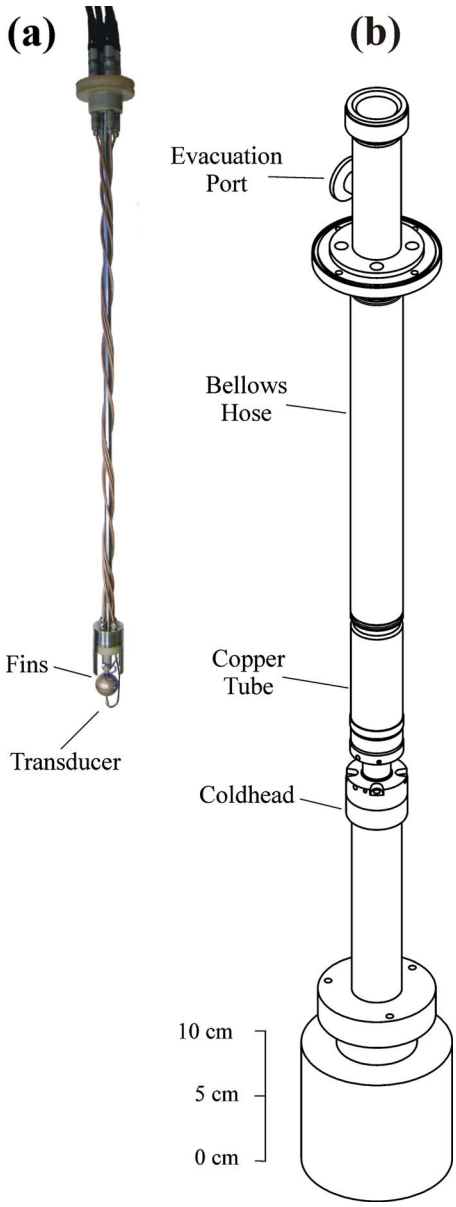

FIG. 5. (Color online) (a) Sample holder insert that slides into the cryostat. Cable leads for the transducer are wrapped around the support tube. Fins provide thermal contact with the inside surface of the copper tube of the cryostat [shown in (b)]. In this picture, a bulk modulus transducer is mounted on the insert, but other types of transducers (see Fig. 1) also can occupy this position. (b) Central core of the cryostat. The evacuation port for the sample chamber, stainless steel bellows, copper tube, and coldhead of the refrigeration system are shown.

A. Construction of the main cryostat

Transducers containing liquid specimens are suspended at the bottom of a sample holder insert, which is shown in Fig. 5(a). This insert consists of a 40-cm-long stainless steel support tube with a wall thickness of 0.1 mm that, at the top

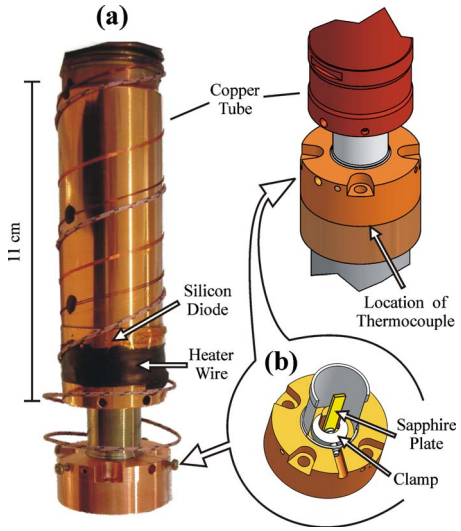

FIG. 6. (Color online) (a) Close-up photograph of the copper tube and diagrams of the housing for the sapphire plate. In the picture, the heater wire for the copper tube is covered by black epoxy. (b) Cutaway drawing of the bottom mount of the sapphire plate. One end of the sapphire plate is gripped by a screw-tightened stainless steel clamp. The thermocouple referred to in the diagram is for monitoring the temperature of the coldhead.

end, is attached to a vacuum plug with feedthroughs for four cables and, at the bottom end, is connected to a nickel-plated partially hollowed out copper cylinder. (All stainless steel parts in the cryostat are made from type 316 stock, and all copper parts are made from oxygen-free high conductivity stock.) When the sample holder insert is placed inside the cryostat [shown in Fig. 5(b) with the outer wall of the vacuum jacket removed], two fins flaring out from the cylinder rub against the inside of the copper tube, which has an inner diameter of 25 mm ± 3 μm. (The ± 3 μm tolerance cited here is extraordinary; all other parts of the cryostat are machined with a tolerance of ± 0.1 mm.) The cylinder caps (albeit not vacuum tight) an enclosure inside the copper tube that is designated as the sample chamber. Normally, the cryostat is operated with the sample chamber filled with gas (air or nitrogen), and most heat is transported between the transducer and the sample chamber through the gas.

Several steps are taken to thermally isolate the sample chamber from the rest of the cryostat. In an effort to minimize conduction of heat from the top of the cryostat, the copper tube is suspended below a 0.1-mm-thick, 258-mm-long, 27.5-mm-i.d. stainless steel vacuum bellows hose. The low thermal conductivity of stainless steel makes it an appropriate material to use here and folds in the bellows more than double the length of the thermal path between the copper tube and the top of the cryostat. Including bellows in the design provides secondary benefits, too; for example, this flexible component relieves strains in the central core arising from thermal expansion or pressure differences in the cryostat. It also makes assembly of the cryostat convenient: The flexibility of the bellows allows one to adjust the length of the central core of the cryostat to fit the outer vacuum jacket. Incidentally, the bellows hose supports the majority of the weight of the copper tube.

Another potential pathway by which heat can be conducted into the sample chamber occurs through the sample holder insert described above. Not much heat is conducted through the support tube since it is constructed of 0.1-mm-thick stainless steel, but a nontrivial amount of heat is conducted through outer braiding and inner wires of four coaxial cables connected to the transducer. Braiding on the cables terminates at the nickel-plated copper cylinder on the bottom of the holder and inner wires of the cables are heat sunk there as well to divert heat from the transducer.

The foremost heat insulation is a vacuum jacket surrounding the central core of the cryostat. The volume between the outer walls of the cryostat and central core of the cryostat is evacuated by a turbopump backed up by an oil-free forepump. A large-bore stainless steel tower is mounted on top of the turbopump to increase the conductance of the vacuum system (the turbopump and vacuum tower are visible in the photograph of Fig. 4). To minimize outgassing, every component (including all screws) of the cryostat and all parts of the vacuum system connected to the cryostat are baked out at 250 °C for 24 h in a chamber evacuated by a forepump. It is recognized, though, that even if the vacuum jacket were thoroughly evacuated, there would remain the problem that heat could be transmitted by thermal radiation. To shield the sample chamber from this source of heating, about 20 reflective Mylar sheets have been wrapped around the copper tube and the stainless steel bellows. The Mylar sheets are attached to the stainless steel bellows hose with aluminum tape to drain off any heat absorbed by this shielding material.

The copper tube is heated by passing a dc electrical current through a nickel-chromium alloy wire that is bonded to the tube. The wire is noninductively wrapped around the tube, that is, counterwound back on itself so that current in the wire does not generate a magnetic field. An epoxy with high thermal conductivity [STYCAST 2850 with catalyst 11 (Grace Specialty Polymers)] is used to bond the wire to the tube. Since the total resistance of the wire in contact with the tube is 30 Ω and it carries a maximum current of 1 A, its maximum heating power is 30 W. The maximum rate at which the temperature of the copper tube can be raised is largely determined by its mass. It takes about 1 min to jump upward by 10 K and between 4 and 5 min to jump upward by 30 K. (However, as described below, more time is required to increase the temperature of the transducer itself.) The copper tube is cooled by a pulse tube cryocooler (Sumitomo Heavy Industries SRP-1512A series), which has a cooling capacity of 5 W at 80 K. The coldhead of the cryocooler is not connected directly to the copper tube; rather, heat is extracted by channeling it through a 3-mm-wide and 2-mm-thick sapphire plate.[16] The advantage of this setup is that the rate of heat extraction is automatically lowered when the sample chamber is near room temperature. If the coldhead were connected directly to the copper tube, the cooling rate at these temperatures would be excessively high (50–60 W) and a commensurately high heating rate from the nickel-chromium alloy wire would be required to stabilize the temperature. Inserting the sapphire plate between the coldhead and the copper tube reduces the cooling rate since thermal conductivity of sapphire is lower by about a factor of 5 at room temperature than at tempera-

tures near 100 K. Thus, the sapphire plate allows us to control temperature much more efficiently using much less cooling and heating powers than otherwise would be required.

In Fig. 6(b), a stainless steel clamp presses the lower end of the sapphire plate against a stub on a copper cylinder that is mounted on top of the coldhead. A thin layer of indium is sandwiched between the sapphire plate and the stub to ensure that they are in firm thermal contact. The upper end of the plate is mounted to the bottom of the copper tube of the sample chamber in a similar manner. Heat is conducted through a 2-cm-long portion of the sapphire plate. The plate is housed inside a 1.6-cm-long, 0.1-mm thin-walled stainless tube to protect it from being twisted and broken as the cryostat is assembled.

The temperature of a transducer mounted in the cryostat is measured by using a silicon diode sensor (shown in Fig. 6). The sensor (Oxford Instruments, part number T1-104) has dimensions of 2×2 mm^2 and is unencapsulated. As Fig. 6(a) shows, the diode is glued to the copper tube, but it is recalibrated to register the temperature of a transducer inserted inside the sample chamber [temperature measurements using a 0.3-mm-diameter negative temperature coefficient (NTC) thermistor bead indicate that, when the sample chamber is filled with air with a temperature of 200 K, the temperature at the position of the transducer is about 0.2 K higher than the temperature of the copper tube]. To determine the temperature of a transducer corresponding to a given forward voltage across the diode, a platinum resistance thermometer is positioned at the spot normally occupied by a transducer, and the sample chamber is flooded with 3-methyl pentane to improve thermal contact between the copper tube and the platinum thermometer (this particular liquid is chosen since it does not undergo phase transitions at our calibration temperatures). The liquid serves to facilitate thermal equilibration within the sample chamber, but we still wait 3 h after changing temperature before making a measurement. Temperatures are measured at several select temperatures in the working range of our cryostat, 94–300 K. The calibration error of the platinum resistance thermometer is smaller than ±0.1 K (traceable to Risø National Laboratory, Denmark).

Our cryostat contains two other temperature sensors. To monitor the coldhead temperature, a type-*J* thermocouple is placed between the coldhead and the copper cylinder mounted on top of the coldhead (location shown in Fig. 6). Another thermocouple is attached to the copper tube to alert the temperature control system if runaway heating should occur. If it senses a temperature above 80 °C, the power to the heater wire is shut off.

B. Temperature control system of the main cryostat

Electronic circuits of the temperature control system perform two basic functions.

(i) Measurement of a voltage across a silicon diode, which, as described above, is calibrated to yield the temperature of a transducer mounted in the cryostat.
(ii) Generation of electrical current for the nickel-chromium alloy heater wire to raise the temperature.

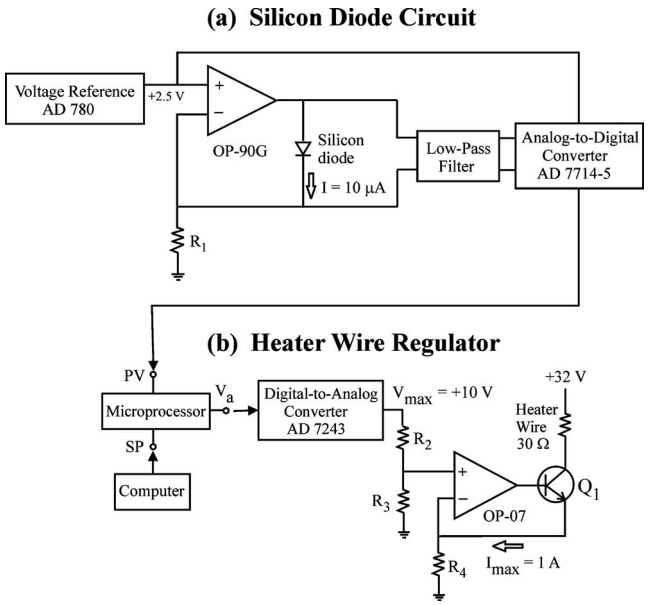

FIG. 7. (a) Functional block diagram of circuits used to measure the forward voltage drop across the silicon diode. Resistor R_1 is 250 kΩ. (b) Functional block diagram of circuit used to generate electrical current in the heater wire. Resistor values are $R_2=9$ kΩ, $R_3=1$ kΩ, and $R_4=1$ Ω. Transistor Q_1 is a TIP 141 Darlington transistor.

Temperature control is implemented by a proportional-integral feedback loop, and temperature can be maintained with high stability only if measurements of the diode voltage are highly precise. However, in order to make precise voltage measurements, the temperature of sensing electronic circuits themselves cannot be allowed to fluctuate. To this end, these circuits are mounted in an enclosure with a well-regulated temperature. The resultant control system is capable of holding the temperature of transducers steady within a few millikelvins over the span of several days or even several weeks.

Figure 7(a) shows electronic circuits used to measure the diode voltage. To improve precision of measurements, a high precision voltage source (AD 780) is used to provide a voltage reference (2.5 V) for components in this circuit. Current for the diode is provided by a precision low-voltage micropower operational amplifier (Analog Devices OP-90 G) and, with the indicated value of R_1 being used in this circuit, this current is 10 μA.

The forward voltage drop across the diode lies between 0.5 and 1.0 V for the operating temperature range of the cryostat, 94–300 K. If the temperature of the diode were stabilized to within a few millikelvins, the diode voltage would fluctuate by a few microvolts; hence, in order to realize this level of stability, we must measure the diode voltage with ppm resolution. This is done by reading the voltage with a 24 bit analog-to-digital converter (Analog Devices AD 7714-5). This chip digitizes the voltage (using sigma-delta or charge balancing conversion) at a selected frequency of 153.6 kHz and then processes the data with a low-pass digital filter. The filter outputs voltage readings with a signal-to-noise ratio on the order of 1 ppm if the filter is programed to issue readings at a rate of 10 Hz. This rate is deemed to be adequate for maintaining temperature control since temperatures of transducers usually change no faster than about

0.1 K/s. One advantage of setting the output rate to 10 Hz is that notches occur at integral multiples of 10 Hz in the filter's frequency response, with the fortunate consequence that 50 or 60 Hz pickup is attenuated by 150 dB. In addition to the low-pass digital filter mentioned above, the circuit contains a second filter—a passive low-pass analog filter—that is installed in front of inputs to the analog-to-digital converter (ADC) to avoid creating aliases, spurious signals caused by improper sampling of high-frequency contributions to the diode voltage. In compliance with the Nyquist criterion of not sampling voltages with frequencies above half the digitizing frequency of the ADC (in this case, 153.6 kHz/2), a cutoff frequency of 10 kHz is chosen for this antialiasing filter.

In order to monitor the transducer temperature with high precision, it is imperative that the temperature of circuits in Fig. 7(a) not be allowed to drift since outputs of the voltage reference, operational amplifier, and ADC all vary with chip temperature. The size of error introduced by drift of chip temperature may be estimated by examining variation of the voltage outputted from the ADC [processing voltage (PV)] as the temperature of the circuits is changed (but with the diode maintained at a constant temperature). When the temperature of the circuits is raised 10 °C, PV changes by 110 μV, corresponding to a temperature misreading of about 50 mK. To avoid this error, circuits in Fig. 7(a) (excluding, of course, the silicon diode) are encased in a metal box and mounted on a Peltier element (Melcor CP1.0-127-05L). The temperature of the circuits is maintained at 28 ± 0.01 °C by an analog temperature regulator that also is mounted on the element. With the temperature of chips stabilized in this manner, a major source of error in the sensing circuitry is eliminated, making it possible to detect millikelvin-sized changes in transducer temperature. This capability distinguishes our temperature control system from many commercial units.

The temperature control system is based upon a feedback control loop. A custom-built microprocessor circuit [Fig. 7(b)] reads the diode voltage (PV) and compares it to an expected value [set point (SP) voltage dictated by a temperature control program running on a PC]. If these voltages do not agree, the microprocessor alters the electrical current flowing in the heater wire in such a way as to move the transducer temperature closer to the desired temperature corresponding to SP. Specifically, it adjusts a voltage V_a that regulates an amplifier supplying current to the heater wire. It is found that best feedback control is realized when this voltage is steered by both the instantaneous error, $E = \mathrm{SP} - \mathrm{PV}$, and integrated values of past errors using the standard proportional-integral (PI) algorithm,[17,18]

$$V_a = K_p\left(E + \frac{1}{T_n}\int_0^t E dt\right), \tag{1}$$

where t is cumulative elapsed time and K_p and $1/T_n$ are the proportionality gain and integral gain parameters, respectively. These two parameters are chosen so that steps in temperature are carried out in a slightly underdamped manner. Temperature can be changed quicker than a critically damped system if we allow temperatures to slightly overshoot the target before settling back to it. When jumping upward by 10 K, it takes about 20 min for error E to settle to zero; when increasing temperature by 30 K, 30 min are required to stabilize the temperature.

The circuit shown in Fig. 7(b) performs the same function as a commercial proportional-integral-derivative (PID) temperature controller, but derivative control is omitted in this particular instance because, with temperature readings being received from the ADC at a rate of 10 Hz, the fastest temperature response that can be determined is only about 1 Hz. This is deemed too slow for derivative control to be beneficial. In contrast, the microregulator temperature controller discussed below in Sec. III is a fully analog system, and the rate of its temperature readings are not limited by digitization. Since it registers much quicker temperature responses, derivative feedback temperature control is employed in that case. (A fuller discussion of PID temperature control is given below in Sec. III B.)

The microprocessor controls the rate at which data is transferred from the ADC to the microprocessor. Data are transmitted along a serial line in synchronization with a clock signal set by the microprocessor. When this clock is set to 2.4 kHz, the 24 bit word containing the PV reading can be transmitted in 10 ms. Since it takes about 30 ms to calculate voltage V_a from the PI algorithm and another 10 ms to translate this voltage into a new heater current, it takes a total of 50 ms to execute a correction of the heater current. This is fast enough to adjust the heater current between each PV reading, for PV readings are available once every 100 ms.

The rest of the circuitry shown in Fig. 7(b) is related to control of current in the heater wire by voltage V_a. This voltage is transformed into an analog signal by a 12 bit digital-to-analog converter (Analog Devices AD 7243), and the maximum output of this chip is 10 V. This represents the upper limit of the regulating voltage, and we wish it to give the maximum current allowed in the heater wire, 1 A. Current for the heater wire originates from operational amplifier OP-07, the output of which is amplified by a factor of 10^4 by a TIP 141 Darlington transistor.

III. SUBCRYOSTAT AND MICROREGULATOR TEMPERATURE CONTROL SYSTEM

The temperature of a liquid sample can be controlled more precisely when a subcryostat is mounted in the main cryostat. This secondary temperature control stage makes it possible to jump between temperatures quicker and maintain temperatures with higher stability. A quick examination of the configuration of the subcryostat (Fig. 8) reveals obvious reasons for these improvements. The most noteworthy feature is that the transducer is placed in immediate contact with a Peltier element, a local source of heating or cooling. This implies that heat can be quickly delivered to or extracted from the sample; moreover, since heat can be exchanged in both directions, corrections to overshooting target temperatures can be implemented quickly. Secondly, geometry of the special transducer used in this setup, the dielectric cell, helps optimize the rate of heat transfer. The fact that liquid is confined to a thin layer sandwiched between copper disks and that heat flows only through the thickness of the liquid

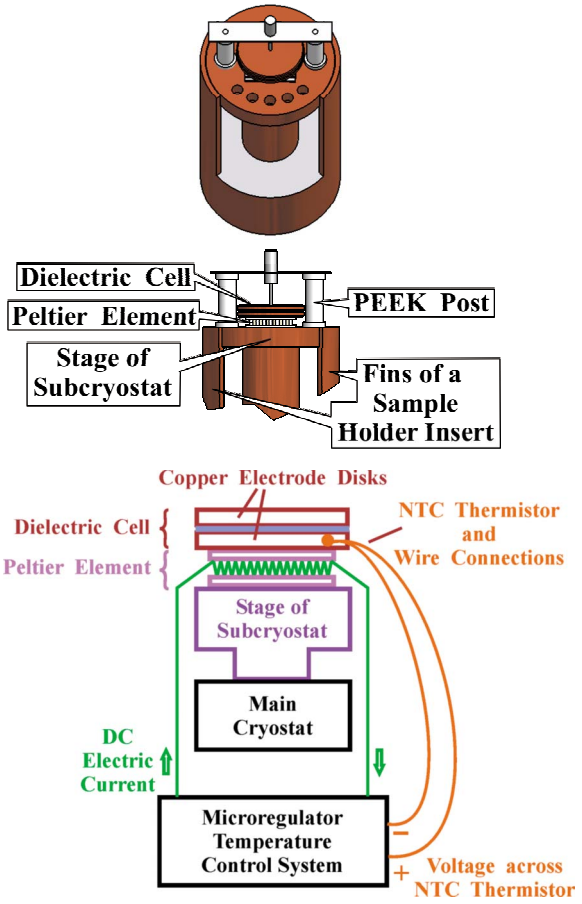

FIG. 8. (Color online) Elements of the subcryostat. Liquid samples are deposited in a 50 μm gap between disks of the dielectric cell. The Peltier element either can heat or cool the dielectric cell, depending on the direction of the electrical current powering the element. The current is controlled by an analog temperature control system that receives temperature feedback information from an NTC thermistor embedded in one disk of the dielectric cell. The orientation of the subcryostat depicted here is convenient for purposes of identifying the various components, but, in reality, the arrangement is inverted, with the main cryostat positioned on top and the dielectric cell placed on the bottom. A gold electrode pin keeps the cell pressed against the Peltier element and provides an electrical connection to one of the copper disks.

means that the liquid does not pose a formidable bottleneck to heat flow [thermal diffusion time $\tau = d^2/D \cong 0.025$ s, where d is the thickness (=50 μm) of the liquid and D is its thermal diffusivity (~ 0.1 mm^2/s)]. Compared to the main cryostat, the thermal resistance of the subcryostat is much lower, and, due to its small mass, its thermal capacitance (heat capacity) is smaller, too. Consequently, the RC thermal relaxation time of the subcryostat is smaller than that of the main cryostat, and corrections in temperature can be implemented much quicker.

Another reason for the quick responsiveness of the system is that electronics governing the current that powers the Peltier element consist entirely of analog circuits. In contrast to the temperature controller for the main cryostat, no limit is placed on the speed of electronics due to a digitization process. Also, the controller used here implements the full PID algorithm, including differentiation action, which increases the speed of response. In keeping with the quick responsiveness of the electronics, an NTC thermistor, noteworthy for its fast thermal response times, is used to measure temperature.

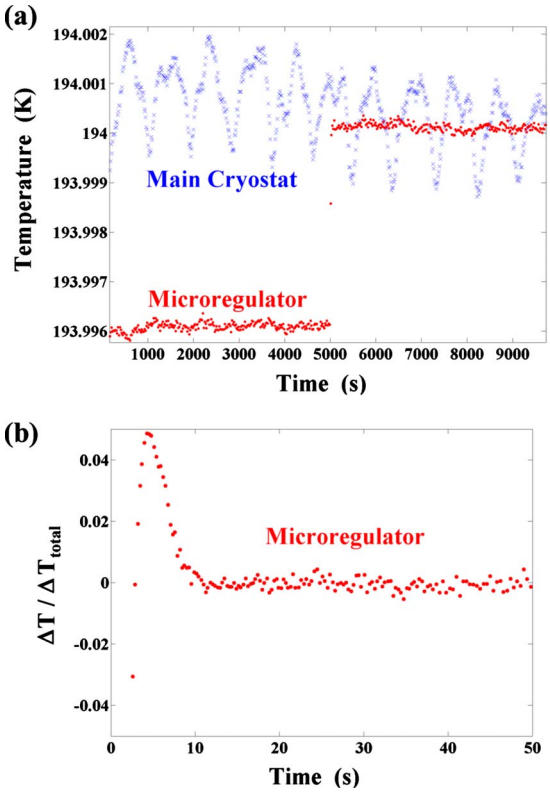

FIG. 9. (Color online) (a) Temperatures of an epoxy sample vs time, as recorded for two cases: (i) temperature is controlled using only the main cryostat (microregulator temperature control is inactive) and (ii) temperature is controlled using the microregulator temperature control system working in tandem with the main cryostat. Data for the two cases are not taken concurrently, but are superposed here for the sake of comparing the two data sets. At the 5000 s mark, the microregulator increases the temperature by 4 mK. (b) Relative change of temperature of a dibutylphtalate sample vs time for the case when temperature is controlled using the microregulator temperature control system working in tandem with the main cryostat. The total temperature change is $\Delta T_{\text{total}} = -0.1$ K (185.6→185.5 K), and it initiates at the 0 s mark. The temperature stabilizes after around 10 s.

Significant improvements in temperature control resulting from using the subcryostat are demonstrated in Fig. 9. Temperatures of an epoxy sample are plotted as a function of time for the two cases of when the microregulator temperature control is turned off and when it is turned on. Temperatures are inferred from measurements of the imaginary part of the capacitance of a dielectric cell containing a thin film of the epoxy. When the microregulator is turned off and temperature is maintained by just the main cryostat, it is seen that temperatures fluctuate by 1–2 mK (measurements are taken after allowing the system to equilibrate for 3 days). However, when the microregulator is turned on, fluctuations are reduced by an order of magnitude. The ability of the system to make quick temperature transitions is evident in Fig. 9(b). It is seen that, after making a jump of −0.1 K, it takes only 10 s for the temperature to stabilize. In contrast, as indicated in Sec. II above, when using the main cryostat alone, it takes several minutes to stabilize the temperature after a jump.

A. Components of the subcryostat

Local heating or cooling of the subcryostat is provided by a Peltier element (Marlow Industries, Part No. MI1022T-

03). The operating principle behind such a device is the Peltier effect (which derives from the property that charge carriers transport thermal energy[19,20]), and it consists of a collection of small blocks of *p*- and *n*-type semiconductor materials (bismuth telluride) that are electrically connected in series and placed between two 1 cm^2 square ceramic plates. When dc electrical current (max $\cong$ 1 A) runs through the semiconductor blocks, heat is transported through the blocks from one ceramic plate to the other. If the electrical current is reversed, heat flow is reversed as well. At room temperature, the maximum heat flow rate for the device is nominally 4.0 W. We estimate that, at temperatures near 200 K, where we typically perform measurements, the maximum heat flow rate is 1–2 W.

One ceramic plate of the Peltier element is thermally connected to the main cryostat in the following manner. As shown in Fig. 8, one side of the Peltier element rests against a cylindrical copper piece that acts as a stage for the subcryostat. To ensure there is a firm thermal connection, the contact area on the stage is covered with the same type of liquid that is being tested in the dielectric cell. (This choice of liquid medium guarantees that thermal conductance does not degrade due to cracks developing in the liquid since, when we carry out measurements, we avoid too low temperatures where cracking might occur.) The stage fits between fins [shown in Fig. 5(a)] of a sample holder insert for the main cryostat (described in Sec. II above), and it is fixed in place with the bottom of the stage thermally connected to the sample holder. The sample holder is inserted into the main cryostat with the entire assembly shown in Fig. 8 inverted upside down.

The dielectric cell transducer that is placed on the other ceramic plate of the Peltier element consists of two 1-mm-thick copper electrode disks with 12 mm diameters. Four Kapton spacers (each with a cross-sectional area of 0.25 mm^2) are inserted between the disks to separate them by about 50 μm. The capacitance of the empty transducer is about 20 pF, the exact value depending upon how much pressure is applied to the spacers. One electrode disk contacts the ceramic plate of the Peltier element with a liquid film inserted between surfaces to ensure there is a good thermal connection. (Again, we use the same type of liquid that is being tested in the dielectric cell. Since liquid films placed on plates of the Peltier element must be changed every time a different liquid is tested in the dielectric cell, the Peltier element is not fixed permanently to either the electrode disk or the subcryostat stage.) As shown in Fig. 8, the whole transducer is pressed against the Peltier element by a gold centering screw which also provides electrical connection to one copper disk. Electrical connection to the other disk is provided by another gold pin that is stuck in a hole drilled in the side of the disk and is not shown in Fig. 8.

An NTC thermistor is used to estimate the temperature of the dielectric cell for purposes of temperature control. A hole is drilled in the copper disk contacting the Peltier element, and a 0.36-mm-diameter glass encapsulated NTC bead thermistor (General Electric thermistor series BR14) is deposited inside and epoxied in place. A thermistor has the advantage of being highly sensitive to temperature

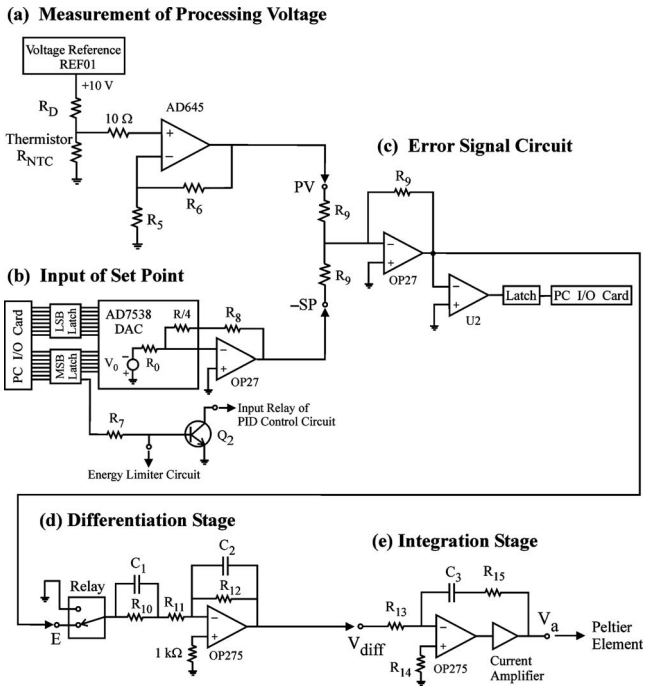

FIG. 10. (a) Circuit that measures processing voltage PV for the microregulator temperature control system. Resistors R_5 and R_6 are 1 and 3 kΩ, respectively. The choice of R_D depends on the temperature: it should be comparable to thermistor resistance R_{NTC}, which varies strongly with temperature. (b) Circuit that establishes set point SP voltage for the microregulator temperature control system. Resistor values are R_7=1 kΩ and R_8 =10 Ω. Q_2 is a 2N2219A-type transistor. (c) Circuit that combines processing voltage PV [output of circuit in Fig. 10(a)] and the negative of the set point SP [output of circuit in Fig. 10(b)] to obtain error signal *E*. Resistor R_9 is 4.7 kΩ. Operational amplifier U2 is used to calibrate the thermistor (see main body of text for details). (d) Differentiation stage of the PID microregulator temperature control system. Resistor values are R_{10}=150 kΩ, R_{11}=12 kΩ, and R_{12}=160 kΩ. Capacitor values are C_1=10 μF and C_2 =10 nF. The input relay to this circuit is activated by transistor Q_2 in Fig. 10(b). (e) Integration stage of the PID microregulator temperature control system. Resistor values are R_{13}=300 kΩ, R_{14}=174 kΩ, and R_{15}=1 MΩ, and capacitance C_3 is 0.66 μF. Resistor R_{14} is included to compensate for input bias current of the operational amplifier, which tends to cause output of the integrator to wander. Details of the current amplifier in the figure are shown in Fig. 11.

changes.[17] It is a semiconductor (a metal oxide), and, as such, its resistance R_{NTC} rises nearly exponentially with decreasing temperature, owing to falling populations of majority charge carriers: $R_{NTC}=R_0(T)\exp(T_a/T)$ (temperature dependence is determined mostly by the exponential factor). Such an exponential form is most appropriate for intrinsic semiconductors (where coefficient T_a corresponds to $E_{gap}/2k_B$, involving band gap energy E_{gap} and the Boltzmann constant k_B), but for an extrinsic semiconductor, such as that used in the thermistor, this expression for resistance serves well as an empirical fitting (called the simplified Steinhart–Hart equation). At working temperatures of our subcryostat, R_0 is typically around 0.1 Ω and T_a is around 2800 K (for example, $R_{NTC}\cong 10^5$ Ω at 200 K).

In the microregulator system described in detail below, temperature is determined not by reading R_{NTC} directly but by measuring a voltage that appears across the thermistor when it is inserted in a voltage divider [see Fig. 10(a) below]. More precisely, temperature is correlated with processing voltage PV, which is four times the voltage across the

thermistor. As discussed below, PV is determined digitally by finding its closest match among a list of voltages stored on a computer. During a calibration process, we ascertain approximately ten pairings of PV and temperature over an approximately 20-K-wide interval, and we perform a best fit of the data using a second order polynomial. We find that this calibration drifts by about 10 mK after 6 months. At present, the voltage divider containing the thermistor must be reconfigured every 20 K or so to measure PV with the highest resolution and to avoid exceeding the maximum voltage that can be read by our circuitry; however, we are in the process of redesigning our circuitry to remove this restriction.

B. Microregulator PID temperature control system

We use a feedback control scheme to determine how electrical current feeding into the Peltier element should be adjusted in order to achieve a desired temperature. As described above, temperature is monitored continuously by measuring the PV, which is equal to four times the voltage across the NTC thermistor. We wish to compare this voltage to a SP voltage corresponding to a target temperature. Deviation from the SP voltage, designated here as error signal $E=\mathrm{SP}-\mathrm{PV}$, is inputted into a standard PID temperature control algorithm,

$$V_a = K_p\left(E + \tau_v \frac{d}{dt}E + \frac{1}{T_n}\int_0^t E dt\right), \tag{2}$$

which gives a voltage regulating an amplifier that supplies current to the Peltier element. Feedback control is based on the raw error (the rate of response of which is set by proportionality gain factor K_p), rate of change of the error (which is included to reduce stability and overshoot problems), and integration of the error (which reduces steady-state errors).[17,18] In contrast to the temperature controller for the main cryostat, derivative feedback control is not omitted here. Also, the PID algorithm is not calculated by a microprocessor but is implemented by an analog circuit. Proportionality gain factor K_p and derivative and integral gain parameters τ_v and $1/T_n$ correspond to combinations of resistors and capacitors, and the procedure for determining optimum values of such components is described below

Figure 10(a) shows how processing voltage PV originates from the thermistor's resistance (R_{NTC}). A voltage drop (V_{NTC}) is established across the thermistor by connecting it in series with resistor R_D and applying ten volts from a precision source (REF01 chip). As discussed above, R_{NTC} varies with temperature, and this causes V_{NTC} to vary, in accordance with the relationship

$$V_{\mathrm{NTC}} = \frac{R_{\mathrm{NTC}}}{R_{\mathrm{NTC}} + R_D} \times 10\ \mathrm{V}. \tag{3}$$

To improve the resolution of this voltage, it is amplified by a noninverting operational amplifier circuit, which, with the values of resistors R_5 and R_6 shown in Fig. 10(a), has a gain of 4. The final output is processing voltage PV that is then compared to the target set point voltage (discussed below).

It should be noted that, since the maximum output voltage of the operational amplifier is 10 V, V_{NTC} cannot exceed 2.5 V (=10 V/4); thus, by Eq. (3) above, R_D must be kept above $3R_{\mathrm{NTC}}$. On the other hand, V_{NTC} cannot be read with high resolution if it is too small, which demands that R_D should not be excessively greater than $3R_{\mathrm{NTC}}$. In practice, we choose different values of R_D that meet these two criteria for certain temperature ranges. For example, at 200 K, a 1 MΩ resistor is used for R_D, but, at temperature of 10 or 20 K below this, a larger resistor is needed since R_{NTC} increases with decreasing temperature.

The other voltage used for temperature regulation is the SP voltage that is stored in a computer. The binary form of the negative of this voltage, −SP, is inputted into the temperature control system as transistor-transistor logic (TTL) signals carried on 14 lines from a programmable input/output interface card of a PC [Fig. 10(b)]. The bit settings are stored in *D*-type latches (74HC573 chips) that then transfer the bit settings to digital-to-analog convertor chip (AD7538). The input binary code [along with a reference voltage (+10 V) supplied to the chip] determines the size of a current issued by the DAC. In conjunction with feedback resistors $R/4$ (which is included in the chip) and R_8, operational amplifier (OP27) converts this current to a voltage, −SP, ranging from $-(16\,383/16\,384)$ 10 V (for binary input 11111111111111_2) to 0 V (for null binary input). One input line from the PC I/O card is used to turn on the transistor switch circuit consisting of resistor R_7 and transistor Q_2. Applying a high TTL signal to resistor R_7 biases the base-emitter junction of transistor Q_2 into forward conduction, which activates the input relay of the differentiation stage in Fig. 10(d). However, should the energy limiter circuit (Fig. 12) be tripped, the base of the transistor will be grounded, thus shutting off its collector current.

Error signal E, equal to $\mathrm{SP}-\mathrm{PV}$, is outputted by a summing amplifier circuit[21] shown in Fig. 10(c). This error signal is produced by operational amplifier (OP27) acting in conjunction with the three R_9 resistors. The other components in Fig. 10(c) are used only during temperature calibration of the thermistor. Since the thermistor is only used to control temperature and we use SPs to set the temperature, it is not necessary to ascertain PV exactly at a given temperature; instead, it suffices to find the nearest value of SP, and with the error signal circuit at our disposal, this is a trivial task: we merely instruct the computer to change the SP voltage outputted by the circuit in Fig. 10(b) until error signal E switches signs. When this occurs, operational amplifier U2 functioning as a comparator[22] here sends a signal to the latch (again, a 74HC573 chip) that then relays a signal to the input/output interface card of the computer to flag the current value of SP as the one closest to PV.

The differentiation part of the PID algorithm is carried out by the circuit shown in Fig. 10(d). The operational amplifier, acting in tandem with capacitor C_1 and resistor R_{12}, outputs a voltage that is proportional to the derivative of error signal E. Acting alone, these components set the output of the operational amplifier to be

$$V_{\text{diff}} = -R_{12}C_1\frac{d}{dt}E. \tag{4}$$

Since noise can cause V_{diff} to wildly fluctuate, it is imperative that differentiation action be rolled off at high frequencies. This is the purpose behind including series resistor R_{11} and shunt capacitor C_2 in the circuit: at frequencies above 1 Hz, the impedance of R_{11} dominates that of capacitor C_1 and differentiation action starts becoming suppressed; at frequencies above 100 Hz, C_2 starts to provide a shunt around resistor R_{12}, and it eventually short circuits V_{diff} to ground at high frequencies. At the other extreme, when the rate of change of E is extremely low, instead of allowing V_{diff} to drop to zero, we wish the output to be proportional to E so that E can be passed along to the subsequent integration stage. For this reason, resistor R_{10} is included; it short circuits capacitor C_1 at low frequencies and cuts off the differentiation action; the operational amplifier instead performs as an inverting amplifier with a gain of about $-R_{12}/(R_{10}+R_{11})$, which contributes to proportionality factor K_p in Eq. (2). With the particular values of components given in Fig. 10(d), this gain happens to be −1.

The integration operation for the PID algorithm is carried out by the circuit shown in Fig. 10(e). The output partially reflects the time integral of input voltage V_{diff}, as revealed by usual analysis of an operational amplifier circuit. Specifically, assuming that the inverting terminal of the operational amplifier is held at a virtual ground, input current I of this circuit equals V_{diff}/R_{13}. This current is related to output voltage V_a by the equation $-dV_a/dt=(I/C_3)+(dI/dt)R_{15}$, which implies

$$V_a = -\frac{R_{15}}{R_{13}}V_{\text{diff}} - \frac{1}{R_{13}C_3}\int_0^t V_{\text{diff}}dt, \tag{5}$$

assuming that the initial input voltage is zero. To express V_a in terms of the error signal, let us substitute the output voltage of the differentiation stage for V_{diff}. In the simplest case, where the rate of change of E is extremely low, V_{diff} is approximately $-ER_{12}/(R_{10}+R_{11})$, and this gives

$$\begin{aligned} V_a &\cong \frac{R_{15}}{R_{13}}\frac{R_{12}}{R_{10}+R_{11}}E + \frac{1}{R_{13}C_3}\frac{R_{12}}{R_{10}+R_{11}}\int_0^t Edt \\ &= \frac{R_{15}}{R_{13}}\left(\frac{R_{12}}{R_{10}+R_{11}}E + \frac{1}{R_{15}C_3}\frac{R_{12}}{R_{10}+R_{11}}\int_0^t Edt\right). \end{aligned} \tag{6}$$

In the more general case, where the time derivative of E is significant, let us substitute in the expression in Eq. (4) as an approximation of the output of the differentiation stage,

$$\begin{aligned} V_a &\cong \frac{R_{15}}{R_{13}}R_{12}C_1\frac{d}{dt}E + \frac{1}{R_{13}C_3}R_{12}C_1\int_0^t \frac{d}{dt}Edt \\ &= \frac{R_{15}}{R_{13}}\left(R_{12}C_1\frac{d}{dt}E + \frac{R_{12}C_1}{R_{15}C_3}E\right), \end{aligned} \tag{7}$$

assuming that the initial error signal is zero. With the particular values of components chosen for these circuits, the coefficients that appear immediately in front of E in Eqs. (6) and (7) are 1 and about 2, respectively. Hence, it is seen that results of the cases represented by Eqs. (6) and (7) nearly follow the general form of the PID algorithm given in Eq. (2), with proportionality gain factor K_p given by R_{15}/R_{13} and derivative and integral gain parameters τ_v and $1/T_n$ given by $R_{12}C_1$ and $(R_{15}C_3)^{-1}$, respectively.

PID parameters K_p, τ_v, and $1/T_n$ are selected so that the system makes temperature changes in a slightly underdamped manner; that is, the temperature overshoots the target temperature, but oscillations decay away rapidly [see Fig. 9(b)]. The advantage of this type of tuning is that the response is faster than a critically damped system. The most practical technique for ascertaining PID parameters that give this behavior is a procedure based upon the Ziegler–Nichols method of controller tuning.[17,18] First, differentiation and integration actions are turned off (capacitor C_3 is replaced by a short circuit and capacitors C_1 and C_2 are removed), and one monitors how the system changes temperature in response to stepping the set point voltage up or down by 10%. Gain K_p is increased until temperature transitions cause the system to oscillate. Half of this value then is chosen as a trial setting for K_p. Next, integration action is reactivated (by replacing capacitor C_3), and $1/T_n$ is increased (by decreasing C_3) until oscillations occur. Again, half of this value then is chosen as a trial setting for $1/T_n$. Then, differentiation action is restored (by reinserting capacitors C_1 and C_2), and the process is repeated for τ_v (which is increased by increasing C_1). Finally, the procedure is repeated with K_p and $1/T_n$ to fine tune their settings.

C. Current amplifier and energy limiter circuits

The heating and cooling sources of the subcryostat, the Peltier element, are powered by the output of the integration stage [Fig. 10(e)]. Operational amplifier (OP275) of this stage cannot by itself supply the current (up to several 0.1 A) that we wish to deliver to the Peltier element, which poses a load of only about 2 Ω; thus, it is necessary to boost the output of the operational amplifier using a current amplifier, the details of which are shown in Fig. 11. This circuit has the configuration of a class AB push-pull power amplifier, and it operates in a similar manner as typical amplifiers described in standard references.[23] One noteworthy characteristic is that steps are taken to avoid crossover distortion. To ensure that at all times either the "current-pushing" (Q_3 and Q_4) or the "current-pulling" (Q_6 and Q_7) emitter follower is activated, we bias base voltages of transistors Q_3 and Q_6 with a dc current flowing through the R_B resistors and the diodes. We also rely on feedback to the operational amplifier to fully activate the emitter followers, and this has the effect of enhancing the dc performance of the amplifier. Hence, by using both dc biasing and operational amplifier feedback to activate the emitter followers, we create an amplifier that has a broad bandwidth. It performs well at both low frequencies and at frequencies that are high enough to ensure quick responsiveness.

The R_E resistors work with transistors Q_5 and Q_8 to establish a maximum current of 400 mA that can be pushed into or pulled from the Peltier element. In addition, we also wish to avoid exchanging high currents (greater than about two-thirds of this maximum current limit) with the Peltier element for too long a period of time. If current flows out of

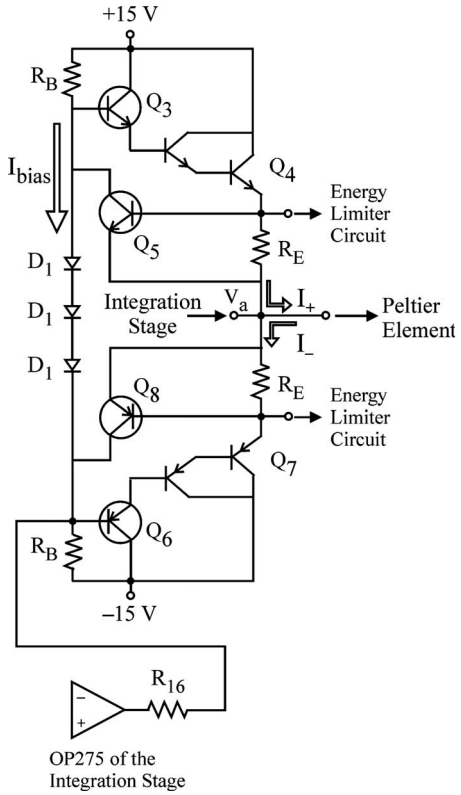

FIG. 11. Current amplifier that provides power to the Peltier element. Positive flowing current I_+, originating from Darlington transistor Q_4 (TIP 120), is pushed into the Peltier element. Negative flowing current I_-, originating from Darlington transistor Q_7 (TIP 125), is pulled from the Peltier element. Transistors Q_5 (BC549C) and Q_8 (BC559C) [acting in conjunction with the pair of R_E (1.5 Ω) resistors] are used to limit these currents to 400 mA and normally are inactive. Transistors Q_3 (2N2222A) and Q_6 (2N2907A) are biased by dc I_{bias} flowing through the pair of R_B (47 kΩ) resistors and the three diodes (IN4148). The amplifier is driven by the output voltage of operational amplifier OP275 [from the integration stage shown in Fig. 10(e)], which is coupled into the circuit through resistor R_{16} (2.2 kΩ).

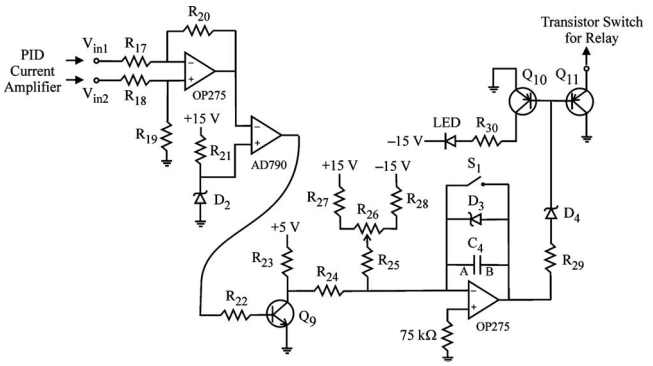

FIG. 12. Energy limiter circuit that restricts the period of time during which high currents are exchanged with the Peltier element. Input voltages $V_{\text{in},1}$ and $V_{\text{in},2}$ monitor the output current of the amplifier in the PID microregulator temperature control system (specifically, these voltages are emitter voltages of transistors Q_4 and Q_7 in Fig. 11). When current sent to or withdrawn from the Peltier element exceeds 260 mA, comparator AD790 turns off transistor Q_9 (2N2222A). This causes charge to build up on capacitor C_4 (=100 μF), and when the voltage drop across the capacitor reaches 10 V, Zener diode D_4 (ZPD10) becomes reverse conducting and transistor Q_{11} (2N2907A) is activated. This turns off transistor Q_2 in Fig. 10(b), and the input relay of the PID circuit in Fig. 10(d) switches to the "off" position, which reduces the current sent to the Peltier element. Resistor values are $R_{17}=R_{18}=1$ kΩ, $R_{19}=R_{20}=10$ kΩ, $R_{21}=3$ kΩ, $R_{22}=1.1$ kΩ, $R_{23}=5.1$ kΩ, $R_{24}=R_{25}=150$ kΩ, $R_{27}=R_{28}=36$ kΩ, $R_{29}=2$ kΩ, and $R_{30}=1.5$ kΩ. R_{26} is a 500 Ω potentiometer. D_2 and D_3 are ZPD3.9-type and ZPD12-type Zener diodes, respectively. Q_{10} and Q_{11} are both 2N2907A-type transistors. S_1 is a manual reset switch.

or into the Peltier element for a prolonged period, we risk damaging the Peltier element by generating too much heat inside this device. Therefore, we have constructed a safety circuit—the energy limiter circuit shown in Fig. 12—that automatically reduces current should it run in excess of 260 mA for a cumulative time of about 30 s. Such a problematic situation arises if the absolute value of error signal E becomes too large, for example, due to attempting to jump to a temperature outside the range covered by certain settings of the microregulator temperature control system or due to an accidental shutdown of the main cryostat.

To simplify the following explanation, let us consider just the case of high current sent to the Peltier element. We monitor the current flowing out of transistor Q_4 in Fig. 11 by monitoring the voltage drop across emitter resistor R_E. Voltages on either side of this resistor are inputted into the energy limiter circuit (the low-side voltage equals the voltage of the emitter of transistor Q_7 since current I_- in Fig. 11 is zero when I_+ is substantial), and a differential amplifier circuit consisting of operational amplifier (OP275) and resistors R_{17} through R_{20} outputs ten times the difference between this pair of voltages. When the monitored current exceeds 260 mA, which is our chosen threshold for activating the energy limiter circuit, this output voltage equals 3.9 V. The output of comparator AD790 (connected to a 3.9 V reference voltage provided by Zener diode D_2 operating in breakdown mode) switches down to ~0.4 V, and this, in turn, shuts off transistor Q_9. Current from the +5 V source, which previously was pulled into the collector of the transistor, now is steered toward capacitor C_4.

This capacitor determines the time at which the energy limiter circuit springs into action and prevents any further high currents from being sent to the Peltier element. Since the timing depends on the amount of charge that accumulates on the capacitor, we take steps to ensure that the capacitor is not initially charged: (i) The presence of diode D_3 guarantees that side B of the capacitor is not positively charged, and (ii) potentiometer R_{26} is adjusted so that any positive charges on side A are bled off by the collector current of transistor Q_9.

Once transistor Q_9 shuts off, the +5 V source feeds a constant current to the capacitor, and positive charge q accumulates on side A of the capacitor at the steady rate, $dq/dt = (+5\text{ V})/(R_{23}+R_{24}) \cong 32\ \mu\text{A}$. Voltage on side B drops at the rate, $-(1/C_4)\times(dq/dt) = -0.322$ V/s, and, after 27 s, this voltage is about −8.8 V, which is negative enough to induce current flow through Zener diode D_4. The reason is that Zener diode D_4 starts conducting in breakdown mode when a reverse voltage of 9.4 V is applied. Since the base voltage of transistor Q_{11} is about 0.6 V [as set by the base voltage of transistor Q_2 in Fig. 10(b)], current starts flowing when voltage on side B equals −8.8 V. When this voltage drops further to about −10 V, current flowing through the diode approaches a level on par with the 32.2 μA current flowing to the capacitor from the 5 V source, and the two currents appreciably cancel each other. Eventually, charge stops accumulating on the capacitor, and voltage on side B ceases drop-

ping. (In any case, this voltage cannot drop much below −11.4 V, the breakdown voltage of Zener diode D_3).

Current flowing through the diode originates from the bases of transistors Q_{10} and Q_{11}. When this current rises to levels described above—on the order of tens of microamperes—the emitter of Q_{11} pulls in all the milliamp-level current originally destined for transistor Q_2 in Fig. 10(b). This is how the energy limiter circuit reduces current sent to the Peltier element: by diverting all the current originally destined for the base of transistor Q_2 in Fig. 10(b) (or equivalently, by grounding its base voltage), this transistor is shut down, and this switches off the input relay of the PID circuit in Fig. 10(d). A light-emitting diode (LED) included in the energy limiter circuit lights up to signify the occurrence of such an event. Transistor Q_{10} is as fully activated as Q_{11} is, and its collector current illuminates the LED. In order to reset the energy limiter circuit and turn on the relay, switch S_1 needs to be momentarily closed. This will neutralize the charge on the capacitor and zero the voltage on side B.

IV. FUTURE IMPROVEMENTS OF THE MICROREGULATOR TEMPERATURE CONTROL SYSTEM

New circuit for measuring the voltage (V_{NTC}) *across the thermistor*. As described in Sec. III A, voltage V_{NTC} is detected in order to monitor the temperature of the dielectric cell in the subcryostat. Currently, this voltage is sampled by inserting the thermistor into a voltage divider circuit. To measure V_{NTC} with high resolution and to avoid exceeding a maximum voltage that can be read by our circuitry, the companion resistor in the divider [R_D in Fig. 10(a)] must be replaced with another one after temperature changes by 20 K or so. As alluded to earlier, we are in the process of redesigning the circuitry to circumvent this task. The voltage divider will be replaced by an inverting operational amplifier circuit with the thermistor inserted in the feedback loop. Electrical current to the thermistor will be provided by a voltage source that can be switched down automatically to a lower voltage when V_{NTC} approaches the maximum output of the operational amplifier. With such a circuit, nothing will need to be changed manually, and it will be possible to collect data over much larger temperature ranges without interruption.

Processing voltage PV will remain proportional to V_{NTC}, although the proportionality factor will no longer be 4. Currently, operators do not have direct access to PV, but the redesigned circuit will include a 24 bit analog-to-digital converter chip that will measure this voltage continuously. This voltage reading will allow us to precisely monitor in real time the temperature of the dielectric cell.

Replacement of the DAC that issues the SP voltage. The SP voltage representing a target temperature is relayed from a computer to the temperature control system through a digital-to-analog converter [see Fig. 10(b) in Sec. III B]. The 14 bit DAC currently in use will be replaced by a 16 bit model. This will boost the resolution of values of SP by a factor of four.

Adjustable proportionality gain factor K_p *in the PID algorithm*. As described in Sec. III B, a feedback scheme based on a PID algorithm is used to control electrical current powering the Peltier element. PID parameters, such as proportionality gain factor K_p, are set by choosing certain resistors and capacitors in Figs. 10(d) and 10(e). The values that we choose give optimum control at a convenient temperature (200 K), but the system does not perform in the same preferred manner at all temperatures because the resistance of the thermistor that is used to monitor temperature does not vary linearly with temperature but, as described in Sec. III A, exponentially rises with inverse temperature. At temperatures well above 200 K, the system is too underdamped, and temperatures oscillate a bit after a jump. As might be inferred from the description of controller tuning in Sec. III B, this behavior signifies that the chosen parameters are too large for these higher temperatures. This problem may be remedied by lowering the proportionality gain factor K_p.

For this reason, we wish to make K_p adjustable, and this can be done most conveniently by inserting a programmable gain amplifier in front of the differentiation stage [Fig. 10(d)]. This modification will multiply the former value of K_p by the gain setting of the amplifier. The problem of the system being too underdamped at high temperatures will be rectified by programing the gain setting to be less than one at these temperatures.

Serial interface with the computer. To prevent electrical noise from being transferred from the computer to the microregulator temperature control system, instructions from the computer will be transferred to the latch chips in Fig. 10(b) of Sec. III B through a serial connection, not through parallel lines of the PC I/O card that currently is in use. An optoisolator can be inserted in a serial line connection to block out noise. This is the same tactic used to hook up the analog-to-digital converter to the microprocessor in the temperature control system for the main cryostat (described in Sec. II B), and the software interface control used in that system will be required here as well.

Stabilized performance of electronic circuits. Output of an electronic circuit can be stabilized significantly if its tem-

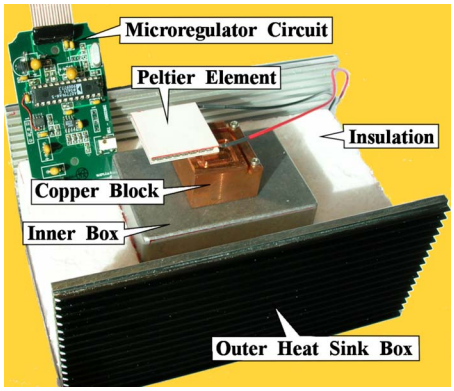

FIG. 13. (Color online) Enclosure for stabilizing the temperature of circuitry of the microregulator temperature system. The circuit board is placed inside the inner aluminum box. Temperature of the box is stabilized by exchanging heat with a Peltier element that is attached to the outer heat sink box. The copper block serves as a thermal conduit between the Peltier element and the inner box, which is packed in Styrofoam insulation.

perature is stabilized. This is demonstrated above (in Sec. II B) with the circuit for measuring the silicon diode voltage in the temperature control system for the main cryostat. As is done with that circuit, we plan to encase the circuitry for the microregulator temperature control system in a metal box and mount it on a Peltier element to stabilize its temperature (Fig. 13).

ACKNOWLEDGMENTS

The authors wish to thank the following staff members and students at Roskilde University for providing helpful information and assistance with diagrams and photographs: H. Hansen, B. Jakobsen, P. Jensen, H. Larsen, A. Nielsen, K. Niss, and Ø. W. Willassen. This work was supported by the Danish National Research Foundation Centre for Viscous Liquid Dynamics "Glass and Time."

[1] I. Gutzow and J. Schmelzer, *The Vitreous State: Thermodynamics, Structure, Rheology, and Crystallization* (Springer, Berlin, 1995).
[2] G. Harrison, *The Dynamic Properties of Supercooled Liquids* (Academic, New York, 1976).
[3] S. Brawer, *Relaxation in Viscous Liquids and Glasses* (American Ceramic Society, Columbus, OH, 1985).
[4] M. D. Ediger, C. A. Angell, and S. R. Nagel, J. Phys. Chem. **100**, 13200 (1996).
[5] C. A. Angell, K. L. Ngai, G. B. McKenna, P. F. McMillan, and S. W. Martin, J. Appl. Phys. **88**, 3113 (2000).
[6] C. Alba-Simionesco, C. R. Acad. Sci., Ser IV: Phys., Astrophys. **2**, 203 (2001).
[7] P. G. Debenedetti and F. H. Stillinger, Nature (London) **410**, 259 (2001).
[8] E. Donth, *The Glass Transition* (Springer, Berlin, 2001).
[9] J. C. Dyre, Rev. Mod. Phys. **78**, 953 (2006).
[10] G. N. Greaves and S. Sen, Adv. Phys. **56**, 1 (2007).
[11] J. Meixner and H. G. Reik, in *Handbuch der Physik*, edited by S. Flügge (Springer, Berlin, 1959), Vol. 3, 413.
[12] N. L. Ellegaard, T. Christensen, P. V. Christiansen, N. B. Olsen, U. R. Pedersen, T. B. Schrøder, and J. C. Dyre, J. Chem. Phys. **126**, 074502 (2007). Matrix equations in the appendix of this paper explicitly demonstrate that the number of independent response functions generally is three.
[13] T. Christensen and N. B. Olsen, Phys. Rev. B **49**, 15396 (1994).
[14] T. Christensen and N. B. Olsen, Rev. Sci. Instrum. **66**, 5019 (1995).
[15] B. Igarashi, T. Christensen, E. H. Larsen, N. B. Olsen, I. H. Pedersen, T. Rasmussen, and J. C. Dyre, Rev. Sci. Instrum. **79**, 045106 (2008).
[16] This technique is suggested to us by another manufacturer of cryocoolers, Aage Christensen.
[17] E. P. Dougherty, in *Encyclopedia of Applied Physics*, edited by G. L. Trigg (VCH, Cambridge, 1997), Vol. 20.
[18] C. D. H. Williams, Feedback and Temperature Control, School of Physics, University of Exeter (http://newton.ex.ac.uk/teaching/CDHW/Feedback/).
[19] N. W. Ashcroft and N. D. Mermin, *Solid State Physics* (Saunders College, Philadelphia, 1976), p. 258.
[20] C. Kittel, *Introduction to Solid State Physics*, 7th ed. (Wiley, New York, 1995), p. 227.
[21] R. M. Marston, *Newnes Linear IC Pocket Book* (Newnes, Oxford, 1997), p. 29.
[22] R. M. Marston, *Newnes Linear IC Pocket Book* (Newnes, Oxford, 1997), p. 17.
[23] For general information about push-pull amplifiers, consult the following references: A. S. Sedra and K. C. Smith, *Microelectronic Circuits* (Holt, Rinehart, and Winston, New York, 1982), pp. 608–614; P. Horowitz and W. Hill, *The Art of Electronics* (Cambridge University Press, London, 1980), pp. 74–77; R. M. Marston, *Newnes Passive and Discrete Circuits Pocket Book* (Newnes, Oxford, 1997), pp. 237–245.